

Accurate and Efficient PSD Computation in Mixed-Signal Circuits: A Time-Domain Approach

Matteo Biggio, Federico Bizzarri, *Senior Member, IEEE*, Angelo Brambilla, and Marco Storace, *Senior Member, IEEE*

I. INTRODUCTION

RADIO-FREQUENCY (RF) circuits have conquered a large portion of the electronic market and mobile devices are largely used every day. One of the key aspects in designing a high-quality RF device is reduction of noise, which requires accurate and efficient simulation in the design phase.

Possibly the most well-assessed time-domain technique to perform this analysis is that referred to as periodic noise analysis (PNOISE) [2], [3], as, for instance, in SPECTRE by CADENCE. This method is grounded on some basic assumptions: (H1) the steady state of the circuit is periodic, (H2) the (cyclo)stationary noise sources effect can be regarded as a small additive perturbation, (H3) the equations describing the circuit can be linearized around the periodic orbit, thus leading to a linear time-varying system called variational model. Linear periodic transfer functions are then used to get the average power-spectral density (PSD) of the electrical variables of interest.

Manuscript received June 21, 2014; accepted August 28, 2014. Date of publication September 10, 2014; date of current version November 1, 2014. This work was supported in part by University of Genoa. This brief was recommended by Associate Editor E. Tlelo-Cuautle.

M. Biggio and M. Storace are with the Department of Electrical, Electronic, Telecommunications Engineering and Naval Architecture, University of Genoa, I-16145 Genova, Italy (e-mail: matteo.biggio@unige.it; marco.storace@unige.it).

F. Bizzarri is with the Dipartimento di Elettronica, Informazione e Bioingegneria, Politecnico di Milano, I20133 Milano, Italy, and also with the Advanced Research Center on Electronic Systems for Information and Communication Technologies E. De Castro (ARCES), University of Bologna, 40125 Bologna, Italy (e-mail: federico.bizzarri@polimi.it).

A. Brambilla is with the Dipartimento di Elettronica, Informazione e Bioingegneria, Politecnico di Milano, I20133 Milano, Italy (e-mail: angelo.brambilla@polimi.it).

As far as (H3) is concerned, this is not the case of mixed-signal circuits, since they are characterized by a discontinuous vector field and discontinuous (digital) variables.¹ In [4]–[6], a unified simulation framework was presented, which allows us to properly define and handle the variational model of these systems. The proposed modeling framework is based on the *saltation matrix* linear operator, a well-known tool to study piecewise-smooth dynamical systems [7]. Several analyses based on the variational model (PNOISE is among those) were thus implemented in the PAN academic circuit simulator.²

As far as (H1) is concerned, there are circuits that do not admit a periodic steady-state solution, e.g., a fractional delta-sigma ($\Delta\Sigma$) phase-locked loop (PLL) with dithering or pulled oscillators. In these cases, one has to resort to the time-domain large-signal noise analysis (e.g., [8] and [9]), where contributions by noise sources to the circuit electrical variables are computed during the numerical solution, without need for a periodic steady state. At the end of this simulation, waveforms can be processed to extract the PSD of noise.³

Large-signal time-domain noise analyses are usually affected by artifacts due to the numerical noise floor of simulators [11] and, to overcome this issue, one could resort to variational time-domain techniques such as the one first proposed in [12]. Aside from being computationally burdensome, the main limitation of this method is the same discussed above concerning (H3), since the approach assumes the analyzed circuits to be well defined in terms of their variational models. Despite that, the approach is interesting and deserves attention since, thanks to the refinements proposed in [1], it allows us to manage noisy electrical variables with generic statistical properties, i.e., stationarity, cyclostationarity or nonstationarity, and to compute average and instantaneous PSDs.

Following this line of reasoning, in this brief, the method defined in [1] and [12] is: i) theoretically extended to analog mixed-signal (AMS) circuits by resorting to the unified simulation framework mentioned above and ii) improved from a numerical efficiency point of view. Two benchmark examples are used to validate the proposed method and to show its capabilities: the ring oscillator analyzed in [1] and a fractional

¹This makes impracticable also the use of frequency-domain noise analysis methods.

²The circuit simulator PAN, developed by the authors and used to derive the results presented in this brief, is available at the URL: <http://brambilla.ws.dei.polimi.it>.

³Among the time-domain methods, the well-known Monte Carlo technique [10] can, of course, be used for all circuits, but it turns out to be extremely time consuming.

$\Delta\Sigma$ PLL with dithering. For the PLL, the obtained results are compared with experimental measurements.

II. STOCHASTIC VARIATIONAL MODEL FOR NOISY MIXED-SIGNAL CIRCUITS

The circuit dynamics are assumed to be described by a nonlinear stochastic differential equation of the type

$$\dot{x}(t) = f(x, t) + g(x, t)\eta(t) \quad (1)$$

where $x(t) \in \mathbb{R}^N$ is the vector of circuit variables, $f : \mathbb{R}^{N+1} \rightarrow \mathbb{R}^N$ is the system vector field (in general nondifferentiable), $g : \mathbb{R}^{N+1} \rightarrow \mathbb{R}^{N \times P}$ is a matrix modeling the noise action on each specific variable, and $\eta(t) \in \mathbb{R}^P$ is a noise vector of white Gaussian stochastic processes [13], modeling the P small amplitude noise sources that are assumed to affect the original circuit. This model is rather general, since any nonpathological circuit described by a differential–algebraic equation can always be recast in this form [14].

The variational approach consists in expressing the solution $x(t)$ (at first order in the noise) as the sum of a noise-free large-signal component $x_s(t)$ and a small-amplitude stochastic component $\xi(t)$. In [12] the variational model was used to implement a noise simulator in time domain, which is able to produce the noise variances and covariances of circuit variables as a function of time, provided that noise models for the devices in the circuit are available. In principle, all those circuits that can be simulated by the transient analysis in a circuit simulator can be handled.

The stochastic variational model of the circuit is described by the following linear time-varying stochastic differential equation (SDE):

$$\dot{\xi}(t) = J(t)\xi(t) + D(t)\eta(t) \quad (2)$$

where $J(t) \equiv \partial_x f(x_s(t), t) \in \mathbb{R}^N$ is the Jacobian matrix and $D(t) \equiv g(x_s(t), t) \in \mathbb{R}^{N \times P}$ is a time-varying incidence matrix reflecting the contribution of η on each one of the N equations of the variational model.

Since (2) is a linear SDE in *narrow sense* [15], for every initial condition $\xi(t_0)$, its solution can be derived as

$$\xi(t) = \Phi(t, t_0)\xi(t_0) + \Phi(t, t_0) \int_{t_0}^t \underbrace{\Phi^{-1}(\tau, t_0)D(\tau)}_{F(\tau)} dW. \quad (3)$$

The integral in (3) is an Ito integral [13], [15], and $\Phi(t, t_0)$ is the *fundamental transition matrix*, obeying

$$\begin{cases} \dot{\Phi}(t, t_0) = J(t)\Phi(t, t_0) \\ \Phi(t_0, t_0) = I_N \end{cases} \quad (4)$$

where I_N is the $N \times N$ identity matrix.

The main limitation of the simulator presented in [12], apart from its computational cost,⁴ is that it assumes the vector

⁴This notwithstanding the noise simulator proposed in [12] implements the Bartels-Stewart algorithm [16], used to solve the Lyapunov matrix equation at each time step.

field f differentiable for $t \geq t_0$ (i.e., the Jacobian matrix $J(t)$ has to be well defined everywhere) and this prevents its use for mixed-signal circuits, in which $J(t)$ is in general not defined at some (*switching* or *impact*) instants $t^{(k)}$. In this context, if at $t^{(k)} > t_0$ $J(t)$ is not well defined, one needs to match $\Phi^-(t^{(k)}, t_0) = \lim_{t \rightarrow t^{(k)-} } \Phi(t, t_0)$ and $\Phi^+(t^{(k)}, t_0) = \lim_{t \rightarrow t^{(k)+} } \Phi(t, t_0)$. This can be done by resorting to a suitable *saltation matrix* $S^{(k)}$, with the property that $\Phi^+(t^{(k)}, t_0) = S^{(k)}\Phi^-(t^{(k)}, t_0)$.

The insertion of saltation matrices in the evolution of $\Phi(t, t_0)$ makes its entries exhibit discontinuities of first type at instants $t^{(k)}$. This is not an issue in defining the stochastic integral in (3), since the deterministic functions involved need just to be square-integrable [17].

During the large-signal time-domain analysis of the noiseless circuit, the $\Phi(t, t_0)$ matrix is computed by taking also into account crossings that cause switching of the vector field or resetting of state variables. Each time $t^{(k)}$ this happens, a proper saltation matrix $S^{(k)}$ is computed and inserted in the matrix product chain that leads to $\Phi(t, t_0)$, in order to regularize the variational model.

III. COMPUTATION OF THE PSD

Generally speaking, we can assume that $\xi(t)$ is a nonstationary process described by (3). For smooth systems, a time-domain technique for computation of PSD for this kind of processes was proposed in [1], on the basis of [18]. Here, we propose a generalization of those results to nonsmooth systems describing mixed-signal circuits with switching times $\{t^{(k)}\}$.

We study first the time evolution of the correlation matrix of the $\xi(t)$ vector, whose entries are defined as $K_{m,n}(t, t') = \langle \xi_m(t)\xi_n(t') \rangle$. In general, we have (see [15])

$$K(t, t') = \Phi(t, t_0)K(t_0, t_0)\Phi^T(t', t_0) + \int_{t_0}^{\min\{t, t'\}} \Phi(t, \tau)D(\tau)D^T(\tau)\Phi^T(t', \tau)d\tau. \quad (5)$$

By assuming $t > t'$, we have

$$\begin{aligned} K(t + dt, t') - K(t, t') &= \{\Phi(t + dt, t_0) - \Phi(t, t_0)\}K(t_0, t_0)\Phi^T(t', t_0) \\ &+ \int_{t_0}^{t'} \{\Phi(t + dt, u) - \Phi(t, u)\}D(u)D^T(u)\Phi^T(t', u)du. \end{aligned} \quad (6)$$

If $t \neq t^{(k)}$, we can then divide by dt and take the limit $dt \rightarrow 0$, hence calculating the derivative at time t

$$\begin{aligned} \partial_t K(t, t') &= \partial_t \Phi(t, t')K(t_0, t_0)\Phi^T(t', t_0) \\ &+ \int_{t_0}^{t'} \partial_t \Phi(t, \tau)D(\tau)D^T(\tau)\Phi^T(t', \tau) \\ &= J(t)K(t, t'). \end{aligned} \quad (7)$$

If $t = t^{(k)}$ for some k , we have instead, using the saltation matrix $S^{(k)}$

$$K(t + dt, t') - K(t, t') = (S^{(k)} - I) K(t, t') \quad (8)$$

or

$$K(t^{(k)+}, t') = S^{(k)} K(t^{(k)-}, t'). \quad (9)$$

By defining the ‘‘cross-spectral density’’ (see [1, Eq. (9)])

$$K'_{n,m}(t, \omega) = \langle \xi_n(t) \Xi_m(t, \omega)^* \rangle \quad (10)$$

where

$$\Xi_n(t, \omega) = \int_0^t e^{-j\omega\tau} \xi_n(\tau) d\tau \quad (11)$$

we then have

$$K'(t, \omega) = \int_0^t e^{j\omega\tau} K(t, \tau) d\tau \quad (12)$$

and, exploiting the equations derived previously for $K(t, t')$, one finds that

$$\begin{cases} \partial_t K'(t, \omega) = J(t) K'(t, \omega) + e^{j\omega t} K(t) \\ K'(t^{(k)+}, \omega) = S^{(k)} K'(t^{(k)-}, \omega) \end{cases} \quad (13)$$

where $K(t)$ is the *covariance matrix*

$$K_{m,n}(t) = \langle \xi_m(t) \xi_n(t) \rangle. \quad (14)$$

According to (5), for $t = t'$, we have

$$K(t) = \Phi(t, t_0) K(t_0) \Phi^T(t, t_0) + \int_{t_0}^t \Phi(t, \tau) D(\tau) D^T(\tau) \Phi^T(t, \tau) d\tau. \quad (15)$$

The dynamical equation for the covariance matrix can be obtained by differentiating (15) with respect to t . This poses no problems as long as $t \neq t^{(k)}$, since $\Phi(t, t')$ is differentiable. Thus, with some algebra, we obtain

$$\dot{K}(t) = J(t) K(t) + K(t) J^T(t) + D(t) D^T(t) \quad (16)$$

where the Jacobian matrix $J(t)$ of the system is well-defined for $t \neq t^{(k)}$. Due to the switching dynamics, when $t = t^{(k)}$, $K(t)$ has a discontinuity. Indeed, expressing $K(t^{(k)+})$ with (15), and since the fundamental matrix solution obeys $\Phi(t^{(k)+}, t') = S^{(k)} \Phi(t^{(k)-}, t')$, it is straightforward to show that

$$K(t^{(k)+}) = S^{(k)} K(t^{(k)-}) S^{(k)T}. \quad (17)$$

According to [1], the PSD can be then calculated as

$$\text{PSD}(\omega) = \lim_{t \rightarrow \infty} \frac{2}{t} \int_0^t \text{Re} \{ K'(\tau, \omega) e^{-j\omega\tau} \} d\tau. \quad (18)$$

Equations (13), (16)–(18) are then a closed system of equations for the PSD at frequency ω .

It is worth noticing that, for each frequency f , the limit in (18) may not converge to a single value if a circuit with arbitrary large signal excitations and nonstationary noise sources is considered [1]. This happens since the computed (and measured) PSD typically depends on time.

IV. NUMERICAL IMPLEMENTATION

Despite the fact that the theoretical extension of the method proposed in [1] and [12] to hybrid dynamical system is relevant by itself, to profitably apply it to AMS circuits it must be rethought from a numerical point of view. As a matter of fact, the PSD calculation based on (18) is numerically cumbersome, since it requires the solution of (13), (16), and (17). For similar reasons, the approach proposed in [1] and [12] has not been widely adopted in circuit simulators.

Here, a practical and numerically efficient method for spectral estimation is proposed, which in the case of ergodic processes relies on a single numerical integration. The method is based on the numerical evaluation of the fundamental transition matrix $\Phi(t, t_0)$. Specifically, we solve (4) by taking into account discontinuities through the saltation matrix. Then, we use (3) to numerically compute $\xi(t)$ and (11) to estimate $\Xi(t, \omega)$. Finally, we evaluate the cross-spectral density (10) for the circuit variables of interest (i.e., for specific pairs m, n) and use (18) PSDs. For ergodic processes the ensemble averages required by (10) can be replaced by time averaging, employing a single realization of the noise input vector $\eta(t)$. For more general processes, the ensemble averages can be efficiently computed by considering multiple realizations in parallel.

We remark that the proposed method can be applied also to nonstationary processes, for which reliable spectral estimation tools are not available in commercial circuit simulators.

With respect to methods for the spectral estimation based on windowing techniques, this method allows in principle to compute the PSD of the signal of interest with arbitrary accuracy.

V. NUMERICAL RESULTS

The numerical simulations described in this section were performed on an INTEL-17 running at 2.6 GHz with LINUX operating system.

A. Ring Oscillator

To compare the results obtained by applying the proposed approach with those reported in [1], we simulated the same benchmark circuit, i.e., the basic ring oscillator shown in Fig. 1. The nonlinear gain of each voltage controlled current source (VCCS) is $f(x) = 0.5I_b \tanh(x/(2\rho V_T))$. The sources of white Gaussian noise are the resistors and the PSD of one of the state variables is computed.⁵

⁵The circuit is totally symmetric hence identical results are obtained considering the three state variables.

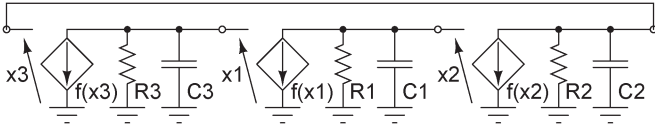


Fig. 1. Schematic of the ring oscillator composed of three identical cells. $R1 = R2 = R3 = 2 \text{ k}\Omega$, $C1 = C2 = C3 = 2 \text{ pF}$, $\rho = 1$, $I_b = 100 \mu\text{A}$, $V_T = 25 \text{ mV}$.

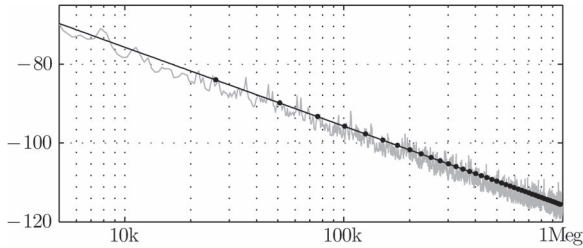


Fig. 2. PSDs of the ring oscillator obtained with different approaches. The black curve and the black dots derive from a PNOISE analysis performed by resorting to PAN and SPECTRE, respectively. The gray curve is obtained with the method presented in this brief. x -axis: frequency offset from the f_0 fundamental of the oscillator [Hz]; y -axis: PSDs [W/Hz] in dBc.

1) *Case $\rho = 1$:* This is the case originally considered in [1]. The circuit is in fact analog and consequently saltation matrices are not necessary. However, since in this case the noise PSD can be determined using PNOISE or the approach of [1], we can compare these methods with the (faster) one proposed in Section IV to test its effectiveness. We first performed a Shooting (SH) analysis and found an accurate numerical approximation of the steady-state solution of the oscillator, obtaining a working frequency of $f_0 = 73.670 \text{ MHz}$ [4], [19], [20]. The working frequency largely depends on the value of the ρ parameter. This circuit was simulated with nominal parameters for 2 ms which allows the determination of the single-sided PSD with offset frequencies up to about 1 kHz. A sequence of 2 799 920 noise samples was generated; the PSD was then computed with the approach outlined in Section IV, implemented as a built-in function in our simulator PAN by exploiting multithread execution. This simulation took 53 s to generate 1996 frequency samples. The obtained result is shown in Fig. 2. The same figure shows also the PSD computed through the PNOISE analysis, implemented in our simulator and in the commercial simulator SPECTRE. The results are in very good agreement and nicely compared with the original [1].

2) *Case $\rho = 10^{-9}$:* To appreciate the capabilities of the extended method, we consider this very small value of the ρ parameter which corresponds to an extremely sharp characteristic of the VCCS. From an analytical point of view the circuit equations remain analog but from a numerical standpoint the VCCSs behave as digital components. In this situation, the insertion of saltation matrices in the time evolution of the fundamental solution matrix is mandatory to achieve meaningful numerical results. In other words, by resorting to the unified simulation framework presented in [4], the PAN circuit simulator is able to insert proper “correction factors” in computing the solution of the system variational problem. So doing, both PNOISE analysis and the approach proposed in this brief

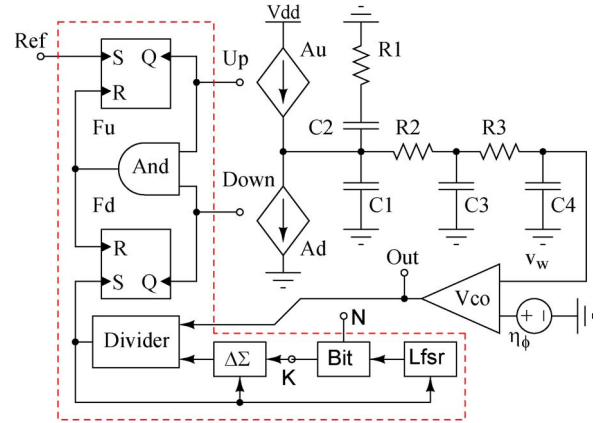


Fig. 3. Schematic of the $\Delta\Sigma$ PLL with dithering. Fixed parameters: $C1 = 6.8 \text{ nF}$, $C2 = 120 \text{ nF}$, $C3 = C4 = 4.7 \text{ nF}$, $R1 = 120 \Omega$, $R2 = R3 = 75 \Omega$, $Au = Ad = 2.25 \text{ mA}$, $K_{vco} = 47 \text{ MHz}$, $f_{ref} = 25 \text{ MHz}$.

can still be applied and it is possible to compare the obtained results.⁶

By performing a SH analysis, the limit cycle exhibited by the oscillator when $\rho = 10^{-9}$ was computed, thus deriving that the working frequency of the oscillator increases to 86.586 MHz. With respect to the spectrum obtained for $\rho = 1$ (see the gray curve in Fig. 2) a shift up of about +3 dB is observed. This result has been compared, showing perfect agreement, with the PNOISE analysis performed with PAN. The derived curves are not reported in Fig. 2 to avoid reducing its readability, since they are very close to the already plotted ones.

B. Fractional $\Delta\Sigma$ PLL With Dithering

To highlight the effectiveness of the proposed approach an interesting and challenging benchmark is considered, a fractional $\Delta\Sigma$ PLL with dithering, whose schematic is shown in Fig. 3. It implements, through a mixed analog/digital modeling approach, the AD4151 commercial PLL by ANALOG DEVICES and the ROS-1800+ voltage controlled oscillator (VCO). This PLL is equipped with both an integer divider and a fractional one but a dithering source is not available to prevent spurs. To compare simulation results, experiments were conducted by using this PLL implemented on the UG-369 evaluation board by ANALOG DEVICES. The frequency measurements were performed through the spectrum analyzer E4440 of AGILENT TECHNOLOGIES. The device was configured as a fractional PLL characterized by a VCO working at 1775.2 MHz, with a reference frequency of 25 MHz and a frequency ratio $70 + N/125$, where the fractional part is obtained by means of a 12-bit $\Delta\Sigma$ modulator setting $N = 26$. In our simulations, the $\Delta\Sigma$ modulator was enhanced, as shown in Fig. 3, by adding a dithering block composed of a 16-bit linear feedback shift register (LFSR) configured to show the maximum length cycle

⁶We remark that, as it was shown, for instance, in [6] for a similar example, this comparison cannot be done by resorting to commercial circuit simulators such as SPECTRE. In fact, even if one succeeded in computing the periodic steady-state solution of the oscillator with the SH method, the fundamental matrix evolution would be computed not correctly since saltation matrices are not inserted. As a consequence, the results provided by the PNOISE analysis, which grounds on such a matrix time evolution, would be wrong.

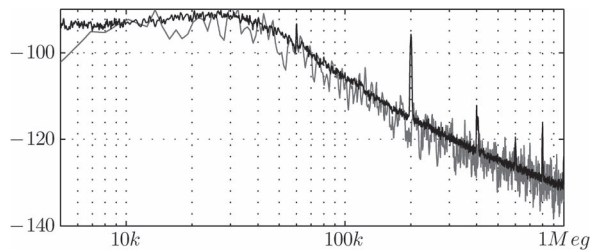


Fig. 4. Simulated (gray) and measured (black) PSDs for the considered PLL. x -axis: frequency offset from the f_0 fundamental of the VCO [Hz]; y -axis: PSDs [W/Hz] in dB.

[21]. The $\Delta\Sigma$ block drives the divider so that on average it divides by a fractional value. The less significant bit of the k input value of the $\Delta\Sigma$ block is set by the bit block that takes as inputs N and the single bit output of the LFSR block. We first simulated the PLL without the dithering block and computed noise effects; the obtained results (not reported) were in good agreement. We then turned on the dithering block and computed once more the noise effect; what we expect is a comparable result but the removal of spurs (located at 200 kHz and multiples) due to the $\Delta\Sigma$ modulator repetition sequence. Since the detailed schematic of the VCO was not available, it was implemented as a *polar oscillator* and its output noise was characterized through a battery of harmonic balance simulations; more details can be found in [22]. The equivalent noise source is represented by the η_ϕ independent voltage source in Fig. 3. The blocks inside the red dashed box are modeled as digital elements through the VERILOG-RTL language. The other elements are modeled as standard SPICE-LIKE elements or as analog behavioral blocks and are noiseless. We first performed a time-domain analysis with noise sources turned off to bring the PLL to work close to the locking condition. Simulation time was reduced by suitably precharging the capacitances of the low-pass filter. We then performed a time-domain noise analysis for 900 μ s: this time corresponds to 25.000 periods of the reference signal and allows the determination of the single-sided PSD with offset frequencies till about 5 kHz far from the fundamental. This simulation took 4100 s. A sequence of 5396577 noise samples was generated and processed by using the proposed approach in 47 s (multithreading, frequency grid composed of 896 points) to generate the PSD reported in Fig. 4. The simulated PSD of the fractional PLL with dithering overlaps very well the experimental result that refers to the real PLL (*without dithering*). It is worth mentioning that since the evolution of the system is aperiodic the PNOISE analysis cannot be adopted.⁷

VI. CONCLUDING REMARKS

This brief takes a step ahead with respect to [12] and [1] from both a theoretical standpoint (generalization of their framework

⁷Actually, for the sake of completeness, one should notice that the dynamic evolution of the circuit is periodic because of the inherent periodicity of the dithering block that is not implemented through a true random numbers generator. At least in principle, one could look for a periodic solution of the dithered fractional PLL but the period would be so long that this approach is impracticable. Consequently, time-domain noise analysis is the only possible solution and aperiodic dynamics is assumed in the whole simulation time.

to AMS circuits) and a numerical standpoint (efficient computation of spectra). The latter aspect has been illustrated through two benchmark examples.

REFERENCES

- [1] V. Vasudevan, "A time-domain technique for computation of noise-spectral density in linear and nonlinear time-varying circuits," *IEEE Trans. Circuits Syst. I, Reg. Papers*, vol. 51, no. 2, pp. 422–433, Feb. 2004.
- [2] M. Okumura, T. Sugawara, and H. Tanimoto, "An efficient small signal frequency analysis method of nonlinear circuits with two frequency excitations," *IEEE Trans. Comput.-Aided Design Integr. Circuits Syst.*, vol. 9, no. 3, pp. 225–235, Mar. 1990.
- [3] R. Telichevesky, K. Kundert, and W. J. , "Efficient AC and noise analysis of two-tone RF circuits," in *Proc. DAC*, 1996, pp. 292–297.
- [4] F. Bizzarri, A. Brambilla, and G. S. Gajani, "Steady state computation and noise analysis of analog mixed signal circuits," *IEEE Trans. Circuits Syst. I, Reg. Papers*, vol. 59, no. 3, pp. 541–554, Mar. 2012.
- [5] F. Bizzarri, A. Brambilla, and G. S. Gajani, "Periodic small signal analysis of a wide class of type-II phase locked loops through an exhaustive variational model," *IEEE Trans. Circuits Syst. I, Reg. Papers*, vol. 59, no. 10, pp. 2221–2231, Oct. 2012.
- [6] F. Bizzarri, A. Brambilla, and G. S. Gajani, "Extension of the variational equation to analog/digital circuits: Numerical and experimental validation," *Int. J. Circuit Theory Appl.*, vol. 41, no. 7, pp. 743–752, Jul. 2013.
- [7] M. Di Bernardo, C. Budd, A. Champneys, and P. Kowalczyk, *Piecewise-smooth Dynamical Systems, Theory and Applications*. London, U.K.: Springer-Verlag, 2008.
- [8] T. Sickenberger and R. Winkler, "Efficient transient noise analysis in circuit simulation," *Proc. Appl. Math. Mech.*, vol. 6, no. 1, pp. 55–58, Dec. 2006.
- [9] E. Buckwar and R. Winkler, "Multistep methods for SDES and their application to problems with small noise," *SIAM J. Numer. Anal.*, vol. 44, no. 2, pp. 779–803, 2006.
- [10] P. Bolcato and R. Poujois, "A new approach for noise simulation in transient analysis," in *Proc. IEEE ISCAS*, May 1992, vol. 2, pp. 887–890.
- [11] M. Biggio, F. Bizzarri, A. Brambilla, and M. Storage, "Effects of numerical noise floor on the accuracy of time domain noise analysis in circuit simulators," in *Proc. IEEE ISCAS*, May 2013, pp. 2694–2697.
- [12] A. Demir, E. Liu, and A. Sangiovanni-Vincentelli, "Time-domain non-Monte Carlo noise simulation for nonlinear dynamic circuits with arbitrary excitations," *IEEE Trans. Comput.-Aided Design Integr. Circuits Syst.*, vol. 15, no. 5, pp. 493–505, May 1996.
- [13] P. E. Kloeden and E. Platen, *Numerical Solution of Stochastic Differential Equations*. Berlin, Germany: Springer-Verlag, 1992.
- [14] L. Chua, C. A. Desoer, and E. S. Kuh, *Linear and Nonlinear Circuits*. New York, NY, USA: McGraw-Hill, 1987.
- [15] L. Arnold, *Stochastic Differential Equations: Theory and Applications*. Hoboken, NJ, USA: Wiley, 1974.
- [16] R. H. Bartels and G. W. Stewart, "Solution of the matrix equation $ax + xb = c$ [4]," *Commun. ACM*, vol. 15, no. 9, pp. 820–826, Sep. 1972.
- [17] N. Privault, *Stochastic Analysis in Discrete and Continuous Settings*. Berlin, Germany: Springer-Verlag, 2009.
- [18] D. Lampard, "Generalization of the Wiener-Khinchine theorem to non-stationary processes," *J. Appl. Phys.*, vol. 25, no. 6, pp. 802–803, Jun. 1954.
- [19] K. Kundert and A. Sangiovanni-Vincentelli, "Simulation of nonlinear circuits in the frequency domain," *IEEE Trans. Comput.-Aided Design Integr. Circuits Syst.*, vol. CAD-5, no. 4, pp. 521–535, Oct. 1986.
- [20] A. Brambilla and G. Storti-Gajani, "Frequency warping in time domain circuit simulation," *IEEE Trans. Circuits Syst. I, Fundam. Theory Appl.*, vol. 50, no. 7, pp. 904–913, Jul. 2003.
- [21] H. Beker and F. Piper, *Cipher Systems: The Protection of Communications*. Hoboken, NJ, USA: Wiley, 1982.
- [22] M. Biggio, F. Bizzarri, A. Brambilla, G. Carlini, and M. Storage, "Reliable and efficient phase noise simulation of mixed-mode integer-N phase-locked loops," in *Proc. ECCTD*, Sep. 2013, pp. 1–4.